One-dimensional topological chains with Majorana fermions in two-dimensional nontopological optical lattices

Lei Jiang, Chunlei Qu, and Chuanwei Zhang

Phys. Rev. A **93**, 063614 — Published 13 June 2016

DOI: 10.1103/PhysRevA.93.063614

1D topological chains with Majorana fermions in 2D non-topological optical lattices

Lei Jiang, Chunlei Qu and Chuanwei Zhang*
Department of Physics, The University of Texas at Dallas, Richardson, Texas 75080, USA

The recent experimental realization of 1D equal Rashba-Dresselhaus spin-orbit coupling (ERD-SOC) for cold atoms provides a disorder-free and highly controllable platform for the implementation and observation of Majorana fermions (MFs), analogous to the broadly studied solid state nanowire/superconductor heterostructures. However, the corresponding 1D chains of cold atoms possess strong quantum fluctuation, which may destroy the superfluids and MFs. In this Letter, we show that such 1D topological chains with MFs may be on demand generated in a 2D/3D non-topological optical lattice with 1D ERD-SOC by modifying local potentials on target locations using experimentally already implemented atomic gas microscopes or patterned (e.g., double or triple well) optical lattices. All ingredients in our scheme have been experimentally realized and the combination of them may pave the way for the experimental observation of MFs in a clean system.

PACS numbers: 03.75.Ss, 05.30.Fk, 03.65.Vf, 67.85.-d

I. INTRODUCTION

Majorana fermions (MFs) [1] obey non-Abelian exchange statistics and are crucial for realizing fault-tolerant topological quantum computation [2–4]. Following initial theoretical proposals [5–10], some possible signatures of MFs have been observed recently in experiments [11–17] using 1D nanowires or ferromagnetic atomic chains on top of an s-wave superconductor and with strong spin-orbit coupling (SOC). However, these signatures are not conclusive because of disorder and other complications in solid state [18–24]. In this context, the recent experimental realization of SOC [25–31] in ultra-cold atomic gases provides a disorder-free and highly controllable platform for observing MFs. In experiments, 1D equal Rashba-Dresselhaus SOC (ERD-SOC) and tunable Zeeman field have been achieved, which, together with the s-wave superfluidity, makes it possible to observe MFs [32–40] in 1D atomic tubes or chains, similar as the nanowire systems.

However, unlike solid state nanowire systems where s-wave superconducting pairs are induced from proximity effects, the superfluid pairing in the 1D atomic chain is self-generated from the s-wave contact interaction, leading to the strong quantum fluctuation that renders the long range superfluid order impossible in the thermodynamic limit. To circumvent this obstacle, quasi-1D systems with multiple weakly coupled uniform chains [41–49] have been studied in both solid state and cold atoms, where transverse tunneling was found to lift the zero energy degeneracy of multiple MFs.

In this paper, we consider a truly 2D non-topological fermionic optical lattice with the experimentally realized 1D ERD-SOC. We raise the question whether single or multiple topological 1D chains supporting MFs can be on demand generated at target locations in such non-topological 2D systems. Generally, a 1D chain in a 2D lattice can be locally modified to satisfy the topological condition for MFs using the recently experimentally realized single site addressing (the atomic gas microscopes) [50–56] or patterned (e.g., double or triple well) optical lattices [57–59]. However, the atom chain is strongly coupled with neighboring chains through transverse tunneling in the 2D system, therefore a naive expectation is that the coupling may destroy the local topological properties and the associated MFs.

Here we show that 1D topological chains with MFs can indeed be generated on demand from 2D non-topological fermionic optical lattices with the experimentally achieved 1D ERD-SOC. Local addressing lasers in atomic gas microscopes can modify the effective local chemical potentials along single or multiple 1D chains, leading to a topological phase transition to generate discrete topological chains that are characterized by non-zero winding numbers and host MFs at chain ends. Multiple MFs in spatially separated multiple topological chains still couple, with the coupling induced zero energy splitting exponentially decaying with the distance of neighboring topological chains. We emphasize that these 1D topological chains are embedded in the true 2D background where the tunnelings along both x and y directions are the same. This is different from previously studied quasi-1D systems where multiple 1D chains are weakly coupled along the transverse direction which usually destroy MFs. Note that similar results apply also to 3D if 1D chains can be locally addressed in a 3D optical lattice. In the weak transverse tunneling region (quasi-1D), the MF coupling is extremely small for two topological chains separated by one or two non-topological chains, making it possible to observe multiple MFs in 2D or 3D double or triple well optical lattices without requiring the single site addressing.

*Corresponding author.
Email: chuanwei.zhang@utdallas.edu

II. MODEL HAMILTONIAN

We consider a spin-1/2 ultra-cold degenerate fermionic gas (spin $\uparrow$ and $\downarrow$) in a 2D square lattice with the lattice size $N = n_x \times n_y$. As shown in the schematic picture Fig. 1, two Raman lasers couple two spin states to induce 1D ERD-SOC along the x-axis. The far-detuned local addressing lasers [50–56] can modify the local potential of the optical lattice along a 1D chain at target locations along the x-direction. Multiple spatially well separated 1D chains can also be generated using additional local addressing lasers. In the 2D lattice, the tight-binding mean-field BdG Hamiltonian is

$$H_{BdG} = H_L + H_{SOC} + H_D + H_\Delta, \tag{1}$$

where $H_L = -\sum_{\mathbf{i},\sigma,\eta} t_\eta \left(C^\dagger_{\mathbf{i},\sigma} C_{\mathbf{i}+\eta,\sigma} + H.c.\right) - \sum_{\mathbf{i},\sigma} \bar{\mu} C^\dagger_{\mathbf{i},\sigma} C_{\mathbf{i},\sigma}$ is the bare Hamiltonian in the 2D lattice with $\eta = \{x, y\}$. The fermionic operator $C^\dagger_{\mathbf{i},\sigma}$ ($C_{\mathbf{i},\sigma}$) creates (annihilates) a particle with spin σ at site $\mathbf{i} = (i_x, i_y)$. We use $\bar{\mu} = \mu - 2t_x - 2t_y$ for the effective chemical potential to match with that in the continuous model. t_x and t_y are the nearest neighbor tunnelings along x and transverse y directions respectively. $H_{SOC} = \alpha \sum_{\mathbf{i}} (C^\dagger_{\mathbf{i},\uparrow} C_{\mathbf{i}-\hat{x},\downarrow} - C^\dagger_{\mathbf{i},\uparrow} C_{\mathbf{i}+\hat{x},\downarrow} + H.c.) + h_z \sum_{\mathbf{i}} (C^\dagger_{\mathbf{i},\uparrow} C_{\mathbf{i},\uparrow} - C^\dagger_{\mathbf{i},\downarrow} C_{\mathbf{i},\downarrow})$ describes the experimentally available 1D ERD-SOC, with the SOC strength α and the Zeeman field h_z. $H_D = \sum_{\mathbf{i},\sigma} V_T(i_y) C^\dagger_{\mathbf{i},\sigma} C_{\mathbf{i},\sigma}$ represents the 1D potential dip with the local potential $V_T(i_y)$, which is generated by local addressing lasers and non-zero only at the i_y chain. $H_\Delta = -\sum_{\mathbf{i}} \Delta_{\mathbf{i}} (C^\dagger_{\mathbf{i},\uparrow} C^\dagger_{\mathbf{i},\downarrow} + H.c.)$ is the mean-field paring Hamiltonian, with the order parameter $\Delta_{\mathbf{i}} = -g\langle C_{\mathbf{i},\downarrow} C_{\mathbf{i},\uparrow}\rangle$ and the on-site interaction strength g. Hereafter we take $t_x = t$ as the energy unit. We solve the corresponding BdG equation self-consistently with the pairing gap equation and fixed chemical potential, following the standard numerical procedure [60–64]. To find the ground state, the order parameter has no constraints and could be complex. We use the box boundary condition for the self-consistent calculation. In practical experiments, there is a weak harmonic confinement that may alter the locations of MFs, but does not change the essential physics [64].

The above BdG Hamiltonian preserves particle-hole symmetry $\Xi H_{BdG} \Xi^{-1} = -H_{BdG}$, where $\Xi = \tau_x \mathcal{K}$, $\tau_x = \tilde{\tau_x} \otimes \tilde{\sigma_0} \otimes \tilde{\rho_0}$, $\tilde{\tau_i}$, $\tilde{\sigma_i}$ are 2×2 Pauli matrices acting on particle-hole and spin spaces respectively, $\tilde{\rho_0}$ is a $N \times N$ identity matrix on the lattice site space, and $\mathcal{K}$ is the complex conjugate operator. If the order parameter Δ_i is real, the Hamiltonian is also real, which preserves a time-reversal like symmetry $\Theta H_{BdG} \Theta^{-1} = H_{BdG}$ with $\Theta = \mathcal{K}$, as well as a chiral symmetry $\mathcal{S} H_{BdG} \mathcal{S}^{-1} = -H_{BdG}$ with $S = \Theta \cdot \Xi = \tau_x$. In this case, the system belongs to the BDI topological class characterized by a $\mathbb{Z}$ topological invariant [65, 66].

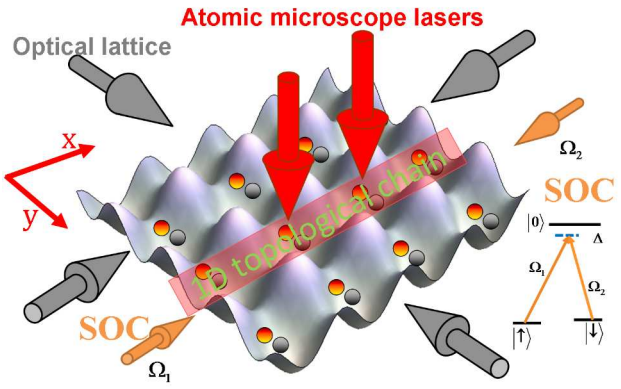

FIG. 1: Illustration of the proposed experimental setup. Grey arrows represent 2D square optical lattice lasers. Red tube demonstrates the 1D potential chain induced by local addressing lasers in atomic microscopes (red arrows). Two counter-propagating Raman lasers (orange arrows) couple two spin states, generating 1D ERD-SOC [25–31].

III. ONE TOPOLOGICAL CHAIN

Since the superfluid order is not stable in strictly 1D systems due to the strong quantum fluctuations [67], the topological analysis fails to work for exact 1D cold atom systems with interactions. This motivates us to extend previous calculations for 1D or quasi-1D [41–49] to truly higher dimensions. To better understand the topological criteria of our 2D system, we first consider a 2D lattice with no tunneling along the y-axis ($t_y = 0$). Thus the 2D lattice is composed of individual x-direction 1D chains. At the central chain we add an extra constant potential $V_T(y_c) = V$, so that the central chain becomes topological, while other parts of the system are still in the non-topological region. Here the topological region is defined locally by the criteria $h_z \geqslant \sqrt{(\mu - V_T)^2 + \triangle^2}$, same as the usual 1D topological chains [7, 10]. In our numerical calculations, we take $n_x = 81$, $n_y = 9$, and $y_c = 5$. In the central topological chain, two MFs should exist at two ends. When t_y is increased from zero to t, the topological chain couples with neighboring non-topological chains and the system changes from 1D to quasi-1D and finally to 2D. A nature question is whether MFs at the center chain will survive with the strong coupling.

Fig. 2 demonstrates the existence of MFs even in truly 2D region with $t_y = t$. The amplitude of the superfluid order parameter $\Delta_{\mathbf{i}}$ is plotted in Fig. 2(a). We find that $\Delta_{\mathbf{i}}$ is homogeneous along the x-axis in the self-consistent calculation, except at the boundary. Furthermore, $\Delta_{\mathbf{i}}$ has a constant phase across on the whole 2D system, therefore we can choose it to be real without loss of generality for the discussion of the topological properties. Fig. 2(b) shows the quasiparticle energy spectrum, where we clearly see the existence of Majorana zero energy modes with a tiny energy splitting $E \approx \pm 2 \times 10^{-5} t$ mainly due to the finite size effect. The mini-gap energy, defined as

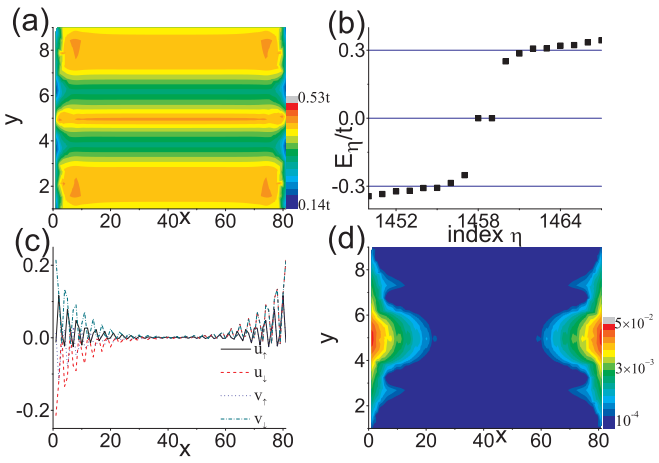

FIG. 2: MFs in a single 1D topological chain in the 2D optical lattice. (a) The amplitude of the order parameter $|\Delta_i|$. (b) The quasiparticle energy spectrum. (c) The zero energy mode wave function along the central chain. (d) The zero energy mode density (Log scale). Parameters: $t_y = t$, $\alpha = 2t$, $g = -5.5t$, $h_z = 1.4t$, $V = -1.45t$, $\mu = -1.555t$.

the energy difference between the zero energy mode and the next lowest quasiparticle state, is comparable to the amplitude of the order parameter Δ_i. Fig. 2(c) shows the wavefunction of the zero energy mode ($E \approx +2 \times 10^{-5}t$ state) along the central chain, which satisfies the relation for MFs: $u_\sigma = \lambda v_\sigma, \lambda = \pm 1$, indicating the central chain is still topological with two MFs at its ends. Fig. 2 (d) shows the density of the zero energy mode, which is square of the zero energy mode wave function for both spin up and spin down atoms in the 2D plane. The zero energy mode still localizes at the ends of the central chain, but slightly spread to neighboring chains which is due to the transverse tunneling. Note that in practical experiments, there exists a finite detuning for the Raman coupling between two bare spin states, which corresponds to an in-plane Zeeman field $h_y\sigma_y$ in our notation. Such non-zero in-plane Zeeman field is known to break the inversion symmetry and lead to the FF type of ground states with finite momentum pairing. We confirm that our results still hold for the FF state. The self-consistent BdG results are present in Fig. 3 which shows the existence of MFs in a single 1D topological chain in the 2D optical lattice with an additional in-plane Zeeman field h_y.

IV. TOPOLOGICAL CHARACTERIZATION

The emergence of MFs at the edges of the central chain originates from the bulk topological properties of the 2D optical lattice with the imprinted 1D topological chain. In the above self-consistent BdG calculations, both the order parameter and the atom density are almost homogeneous along the x-axis, therefore it would be a good

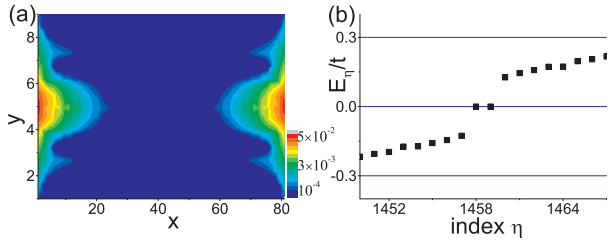

FIG. 3: (a) The zero energy mode density (Log scale). (b). The quasiparticle energy spectrum. $h_y = 0.2t$, the other parameters are the same as Fig. 2.

approximation to assume that the bulk is uniform in the x direction. With a periodic boundary condition along the x-axis, the momentum k_x is a good quantum number. The 2D lattices can be taken as a series of individual 1D chains coupled through transverse tunneling, with the effective BdG Hamiltonian

$$H_{BdG}(k_x) = H_0(k_x)\rho_0 + (V\tau_z\sigma_0 + \triangle'\tau_y\sigma_y)\rho' - t_y\tau_z\sigma_0\rho_x, \quad (2)$$

where $H_0(k_x) = [-2t_x \cos k_x - \bar{\mu}]\tau_z\sigma_0 + 2\alpha \sin k_x \tau_z\sigma_y + h_z\tau_z\sigma_z + \Delta_0\tau_y\sigma_y$ describes the original uniform individual chains with the SOC and the Zeeman field. ρ spans the y-axis chain space with ρ_0 as the identity matrix. $(\rho')_{ij} = 1$ for $i = j = y_c$ and 0 otherwise, $(i, j = 1 \cdots n_y)$. The ρ' part describes the potential and the order parameter differences of the central chain from others. The ρ_x term describes the y-axis hopping between nearest neighboring chains, with $(\rho_x)_{i,j} = 1$ for $|i - j| = 1$ and 0 for others.

The topological properties of the BdG Hamiltonian (2) can be characterized by the winding number W. For a single 1D chain in the 2D optical lattice, the BdG Hamiltonian is in the BDI topological class with a chiral symmetry $SH_{BdG}(k_x)S^{-1} = -H_{BdG}(k_x)$, where $S = \tau_x$. Therefore the BdG Hamiltonian can be transformed to be off-diagonal in the τ space

$$UH_{BdG}U^+ = \begin{bmatrix} 0 & A(k_x) \\ A^T(-k_x) & 0 \end{bmatrix} = h(k_x)\tau_x + d\tau_y \quad (3)$$

by a unitary transformation $U = e^{-i(\pi/4)\tau_y}$, where $A(k_x) = h(k_x) - id$, $h(k_x) = \{[-2t_x \cos k_x - \bar{\mu}]\sigma_0 + 2\alpha \sin k_x\sigma_y + h_z\sigma_z\}\rho_0 - t_y\sigma_0\rho_x + V\sigma_0\rho'$, and $d = \Delta_0\sigma_y\rho_0 + \triangle'\sigma_y\rho'$. The winding number is

$$W = -\frac{i}{\pi}\int_{k_x=0}^{\pi} \frac{dz}{z(k_x)}, \quad (4)$$

where $z(k_x) = \det A(k_x)/|\det A(k_x)|$ [68].

Fig. 4 shows the change of the topological properties with the potential V along the central chain. When V is small, the whole lattice, including the center chain, is in the non-topological region. The corresponding complex value of z rotates when k_x changes from 0 to $k_x = \pi$ as shown in Fig. 4 (a), indicating $W = 0$. When the potential depth $|V|$ increases beyond a threshold value $V_c \approx -t$, W changes to -1. Across V_c, the band

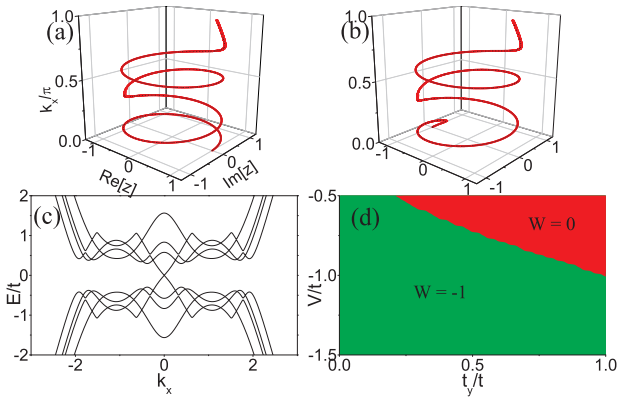

FIG. 4: Complex value z as the function of k_x in the region $(0, \pi)$ with (a) $V = -0.8t$ (non-topological) and (b) $V = -1.2t$ (topological). The other parameters: $t_y = t$, $\alpha = 2t$, $\Delta_0 = 0.4t$, $h_z = 1.4t$, $\triangle' = 0.1t$, $\mu = -1.555t$. (c) The band structure at the topological phase transition point $V = -t$. (d) The winding number as a function of V and t_y.

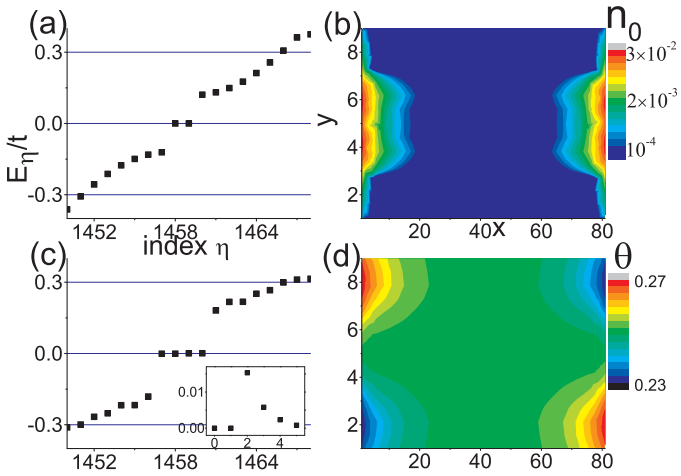

FIG. 5: MFs in two topological chains at $y = 4$ and $y = 6$ (a),(b) or at $y = 2$ and $y = 8$ (c),(d). (a) The quasiparticle energy spectrum for two topological chains separated by one non-topological chain. (b) The zero energy mode density (Log scale). (c) The quasiparticle energy spectrum for two topological chains separated by five non-topological chains. The inset plots the lowest positive quasiparticle energy as a function of the number of non-topological chains in between. (d) The phase of the order parameter $\Delta_\mathbf{i}$. $t_y = t$, the other parameters are the same as Fig. 2.

gap closes (Fig. 4 (c)) and reopens, indicating a topological phase transition to a phase where the central chain becomes topological and hosts a pair of Majorana fermions, agreeing with the self-consistent calculation. This topological phase transition also relies on dimensionality which is controlled by the transverse hopping strength. Fig. 4 (d) illustrates the winding number as a function of the potential depth V and transverse hopping strength t_y. The larger transverse hopping, the deeper central chain potential is needed to move into the topological region with a finite winding number.

V. MULTIPLE TOPOLOGICAL CHAINS

Multiple topological chains may be generated using additional local addressing lasers to obtain multiple MFs. We first consider two topological chains separated by one non-topological chain, with the extra potential V_T adding at $y = 4$ and $y = 6$. The energy spectrum from the self-consistent BdG calculation is plotted in Fig. 5 (a), showing one zero energy mode although there are two topological chains. This is due to the strong coupling between two chains, leading to the winding number $W = -1$, instead of -2. Therefore there is only one pair of MFs when two chains are close. Fig. 5 (b) shows the density of the zero energy mode, which widely spreads along the y-axis from $y = 4$ to $y = 6$.

When two topological chains are further separated by more than one non-topological chains, the analysis of the bulk topological properties based on constant order parameter phase shows that $W = -2$, indicating two pairs of MFs. The effect of adding more non-topological chains between topological ones on the winding number is similar as decreasing the transverse hopping strength. Both situations give winding number $W = -2$ and have multiple degenerate MFs within the assumption of constant value of the order parameter phase. However, in the self-consistent calculation, the order parameter phase is no longer uniform due to the interaction between two MFs at the same end, leading to the splitting of the zero energy states. In Fig. 5 (c), we plot the quasiparticle energy spectrum for two topological chains located at $y = 2$ and $y = 8$ obtained from the self-consistent calculation. Fig. 5 (d) shows the phase $\theta(x, y)$ of the order parameter $\Delta_\mathbf{i} = |\Delta|e^{i\theta(x,y)}$, which has an antisymmetric structure between two topological chains. The phase difference between two ends of one topological chain is opposite to the one on the other topological chain.

In principle there should be no zero energy modes left due to the interaction between MFs, which splits the energy away from zero to a finite value [44, 45]. In practice, due to the large distance between two topological chains, the coupling strength between two MFs on different topological chains is extremely small and the energy splitting becomes negligible. For instance, the five chain separation in Fig. 5 (c) leads to an energy splitting $E \approx 8{\times}10^{-4}t$. The inset in Fig. 5 (c) shows the change of the splitting with the number of non-topological chains between two topological ones. When the number is 0 and 1, $W = -1$, and the splitting is almost zero since there is only one MF at each end. When the number is 2 and above, the winding number becomes -2 and the interaction of two MFs induces a splitting. The energy splitting decreases exponentially with the distance between two topological chains and approaches almost zero for the 5 lattice separation. The above discussions illus-

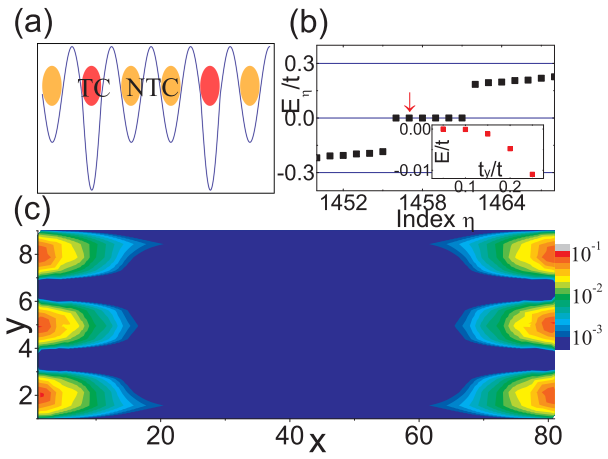

FIG. 6: MFs in quasi-1D triple-well superlattices. (a) Illustration of the triple-well superlattices along the y-axis. Topological chains (TC) are at $y = 2$, $y = 5$ and $y = 8$, separated by non-topological chains (NTC). (b) The quasiparticle energy spectrum showing three pairs of zero energy modes. The insert shows the energy of the second MF mode (pointed by the red arrow) as a function of transverse hopping strength t_y. (c) The zero energy modes density (Log scale). Other parameters $t_y = 0.1t$, $\alpha = 0.75t$, $g = -3.5t$, $h_z = 0.7t$, $V = -0.55t$, $\mu = -0.55t$.

trate that the MF coupling issue in weakly coupled topological chains [43–45] is well resolved by separating the topological chains with non-topological ones. Therefore, with experimentally already realized single-site addressing techniques, we can look for MFs in a truly 2D system, although the underlying spin-orbit coupling is only 1D.

VI. MULTIPLE MFS IN SUPERLATTICES

The interaction between MFs in topological chains can also be significantly reduced by decreasing the tunneling along the transverse direction, which makes the system quasi-1D, instead of 2D. In this case, no large separation between neighboring topological chains is needed, making it possible to generate multiple MFs using patterned optical superlattices along the y-axis. In experiments, optical superlattices such as double well or triple well lattices can be generated using the superposition of different lattice beams [57–59], which are much easier than the single site addressing. Fig. 6 (a) shows a triple well optical lattice along the y-axis with one of the triple wells in the topological region (i.e., two neighboring topological chains separated by two non-topological chains). With a small transverse tunneling $t_y = 0.1t$, the energy splitting for the MF zero energy state is as tiny as $E \approx 5 \times 10^{-5}t$, as shown in Fig. 6. In our calculation, we put three topological chains at $y = 2$, $y = 5$ and $y = 8$, and find one pairs of MFs formed at each topological chain ends. However, if the transverse hopping strength t_y is big, these three topological chains will couple strongly with each other. The inset of Fig. 6 (b) shows the energy splitting of the second pair of MFs with increasing t_y. In the large transverse hopping case ($t_y > 0.1t$), the system leaves only one pair of MFs [45]. We also confirm that similar physics occurs if another triple well superlattice is applied along the z-axis to form a 3D lattice with weak tunneling along both y and z directions.

VII. CONCLUSION

We show that, with the assistant of atomic gas microscopes or patterned optical super-lattices, 2D non-topological optical lattices with experimentally achieved 1D ERD-SOC can host non-coupled 1D topological chains with MFs. We emphasize that although we illustrate the idea using a 2D geometry, the same physics also applies to 3D non-topological optical lattices, providing selected 1D chains can be locally modified or patterned optical superlattices are used. All ingredients in our proposed schemes are available in current experiments, and the scheme may lead to unambitious experimental signature of the long-sought MFs in a clean cold atomic system.

Acknowledgments

This work is supported by ARO (W911NF-12-1-0334), NSF (PHY-1505496) and AFOSR (FA9550-13-1-0045).

[1] F. Wilczek, Nat. Phys. **5**, 614 (2009).
[2] C. Nayak, S. H. Simon, A. Stern, M. Freedman, and S. Das Sarma, Rev. Mod. Phys. **80**, 1083 (2008).
[3] X. Qi and S. Zhang, Rev. Mod. Phys. **83**, 1057 (2011).
[4] M. Z. Hasan and C. L. Kane, Rev. Mod. Phys. **82**, 3045 (2010).
[5] L. Fu and C. L. Kane, Phys. Rev. Lett. **100**, 096407 (2008).
[6] C. Zhang, S. Tewari, R. M. Lutchyn, and S. Das Sarma, Phys. Rev. Lett. **101**, 160401 (2008).
[7] J. D. Sau, R. M. Lutchyn, S. Tewari, and S. Das Sarma, Phys. Rev. Lett. **104**, 040502 (2010).
[8] J. Alicea, Phys. Rev. B **81**, 125318 (2010).
[9] R. M. Lutchyn, J. D. Sau and S. Das Sarma, Phys. Rev. Lett. **105**, 077001 (2010).
[10] Y. Oreg, G. Refael, and F. von Oppen, Phys. Rev. Lett. **105**, 177002 (2010).
[11] V. Mourik *et al.*, Science **336**, 1003 (2012).
[12] M. T. Deng *et al.*, Nano Letter **12**, 6414 (2012).
[13] A. Das *et al.*, Nature Physics **8**, 887 (2012).
[14] L. P. Rokhinson, X. Liu and J. K. Furdyna, Nature Physics **8**, 795 (2012).

[15] M. Veldhorst *et al.*, Nature materials **11**, 417 (2012).
[16] A. D. K. Finck, D. J. Van Harlingen, P. K. Mohseni, K. Jung, and X. Li, Phys. Rev. Lett. **110**, 126406 (2013).
[17] S. Nadj-Perge *et al.*, Science **346**, 602 (2014).
[18] G. Kells, D. Meidan, P. W. Brouwer, Phys. Rev. B (R) **86**, 100503 (2012).
[19] J. Liu, A. C. Potter, K.T. Law, P. A. Lee, Phys. Rev. Lett. **109**, 267002 (2012).
[20] S. Das Sarma, J. D. Sau, T. D. Stanescu, Phys. Rev. B **86**, 220506 (2012).
[21] E. J. H. Lee *et al.*, Phys. Rev. Lett. **109**, 186802 (2012).
[22] D. I. Pikulin, J. P. Dahlhaus, M. Wimmer, H. Schomerus, C. W. J. Beenakker, New J. Phys. **14**, 125011 (2012).
[23] H. O. H. Churchill *et al.*, Phys. Rev. B **87**, 241401 (2013).
[24] E. J. H. Lee *et al.*, Nature Nanotech. **9**, 79 (2014).
[25] Y.-J. Lin, K. J. Garcia and I. B. Spielman, Nature **471**, 83 (2011).
[26] J.-Y. Zhang *et al.*, Phys. Rev. Lett. **109**, 115301 (2012).
[27] C. Qu, C. Hamner, M. Gong, C. Zhang, and P. Engels, Phys. Rev. A **88**, 021604(R) (2013).
[28] A. J. Olson *et al.*, Phys. Rev. A **90**, 013616 (2014).
[29] P. Wang *et al.*, Phys. Rev. Lett. **109**, 095301 (2012).
[30] L.W. Cheuk *et al.*, Phys. Rev. Lett. **109**, 095302 (2012).
[31] R. A. Williams, M. C. Beeler, L. J. LeBlanc, K. Jiménez-García, and I. B. Spielman, Phys. Rev. Lett. **111**, 095301 (2013).
[32] M. Sato, Y. Takahashi, and S. Fujimoto, Phys. Rev. Lett. **103**, 020401 (2009).
[33] S.-L. Zhu, L.-B. Shao, Z. D. Wang, and L.-M. Duan, Phys. Rev. Lett. **106**, 100404 (2011).
[34] K. J. Seo, L. Han, and C. A. R. Sá de Melo, Phys. Rev. Lett. **109**, 105303 (2012).
[35] M. Gong, G. Chen, S. Jia, and C. Zhang, Phys. Rev. Lett. **109**, 105302 (2012).
[36] X.-J. Liu, L. Jiang, H. Pu, and H. Hu, Phys. Rev. A **85**, 021603(R) (2012).
[37] L. Jiang *et al.*, Phys. Rev. Lett. **106**, 220402 (2011).
[38] R. Wei and E. J. Mueller, Phys. Rev. A **86**, 063604 (2012).
[39] X.-J. Liu, Z.-X. Liu, and M. Cheng, Phys. Rev. Lett. **110**, 076401 (2013).
[40] D.-L. Deng, S.-T. Wang, K. Sun, and L.-M. Duan, Phys. Rev. B **91**, 094513 (2015).
[41] M. Wimmer, A. R. Akhmerov, M. V. Medvedyeva, J. Tworzydło, and C. W. J. Beenakker, Phys. Rev. Lett. **105** 046803 (2010).
[42] S. Tewari, T. D. Stanescu, J. D. Sau, and S. Das Sarma, Phys. Rev. B **86**, 024504 (2012).
[43] C. Qu, M. Gong, Y. Xu, S. Tewari, and C. Zhang, Phys. Rev. A **92**, 023621 (2015).
[44] Y. Li, D. Wang, and C. Wu, New J. Phys. **15**, 085002 (2013).
[45] D. Wang, Z. Huang, and C. Wu, Phys. Rev. B **89**, 174510 (2014).
[46] T. Mizushima and M. Sato, New J. Phys. **15**, 075010 (2013).
[47] I. Seroussi, E. Berg, and Y. Oreg, Phys. Rev. B **89**, 104523 (2014).
[48] Arbel Haim, Anna Keselman, Erez Berg, and Yuval Oreg, Phys. Rev. B **89**, 220504(R) (2014).
[49] Ryohei Wakatsuki, Motohiko Ezawa, and Naoto Nagaosa, Phys. Rev. B **89**, 174514 (2014).
[50] P. Würtz, T. Langen, T. Gericke, A. Koglbauer, and H. Ott, Phys. Rev. Lett. **103** 080404 (2009).
[51] W. S. Bakr, J. I. Gillen, A. Peng, S. Föling and M. Greiner, Nature **462**, 74 (2009).
[52] W. S. Bakr *et al.*, Science **329**, 547 (2010).
[53] J. F. Sherson *et al.*, Nature **467** 68 (2010).
[54] C. Weitenberg *et al.*, Nature **471**, 319 (2011).
[55] E. Haller *et al.*, Nature Physics **11**, 738 (2015).
[56] L. W. Cheuk *et al.*, Phys. Rev. Lett. **114**, 193001 (2015).
[57] J. Sebby-Strabley, M. Anderlini, P. S. Jessen, and J. V. Porto, Phys. Rev. A **73**, 033605 (2006).
[58] S. Fölling *et al.*, Nature **448**, 1029 (2007).
[59] C. J. Kennedy, G. A. Siviloglou, H. Miyake, W. C. Burton, and W. Ketterle, Phys. Rev. Lett. **111**, 225301 (2013).
[60] C. Qu *et al.*, Nature Communications **4**, 2710 (2013).
[61] Y. Xu, C. Qu, M. Gong, and C. Zhang, Phys. Rev. A **89**, 013607 (2014).
[62] C. Qu, M. Gong, C. Zhang, Phys. Rev. A **89**, 053618 (2014).
[63] Y. Xu, L. Mao, B. Wu, and C. Zhang, Phys. Rev. Lett. **113**, 130404 (2014).
[64] L. Jiang, E. Tiesinga, X.-J. Liu, H. Hu, and H. Pu, Phys. Rev. A **90**, 053606 (2014).
[65] A. P. Schnyder, S. Ryu, A. Furusaki, and A. W. W. Ludwig, Phys. Rev. B **78**, 195125 (2008).
[66] J. C. Y. Teo and C. L. Kane, Phys. Rev. B **82**, 115120 (2010).
[67] E. Zhao and W. Vincent Liu, Phys. Rev. A **78**, 063605 (2008).
[68] S. Tewari, J. D. Sau, Phys. Rev. Lett. **109**, 150408 (2012).